

Ab initio molecular dynamics study of pressure-induced phase transition in ZnS

This article has been downloaded from IOPscience. Please scroll down to see the full text article.

2006 J. Phys.: Condens. Matter 18 9483

(<http://iopscience.iop.org/0953-8984/18/41/015>)

View [the table of contents for this issue](#), or go to the [journal homepage](#) for more

Download details:

IP Address: 129.252.86.83

The article was downloaded on 28/05/2010 at 14:24

Please note that [terms and conditions apply](#).

Ab initio molecular dynamics study of pressure-induced phase transition in ZnS

Israel Martinez and Murat Durandurdu

Department of Physics, University of Texas at El Paso, El Paso, TX 79968, USA

Received 9 May 2006, in final form 11 September 2006

Published 29 September 2006

Online at stacks.iop.org/JPhysCM/18/9483

Abstract

The pressure-induced phase transition in zinc sulfide is studied using a constant-pressure *ab initio* technique. The reversible phase transition from the zinc-blende structure to a rock-salt structure is successfully reproduced through the simulations. The transformation mechanism at the atomistic level is characterized and found to be due to a monoclinic modification of the simulation cell, similar to that obtained in SiC. This observation supports the universal transition state of high-pressure zinc-blende to rock-salt transition in semiconductor compounds. We also study the role of stress deviations on the transformation mechanism and find that the system follows the same transition pathway under nonhydrostatic compressions as well.

1. Introduction

The pressure-induced phase transitions from fourfold coordinated zinc-blende (ZB) to sixfold coordinated rock-salt (RS) structures have been studied extensively for decades, but clear evidence about the transformation mechanism of this simple phase transition at the atomistic level could not be obtained until recently. A molecular-dynamics (MD) simulation using an interatomic potential [1] revealed that the ZB-to-RS transformation of SiC is due to a cubic to monoclinic unit-cell transformation such that the Si and C sublattices shift with respect to each other along the [100] direction in the ZB structure. Furthermore, the transformation proceeds continuously without any bond breaking, in contrast to the transformation mechanism based on a rhombohedral $R3m$ intermediate state proposed in a first-principles calculation [2]. Motivated by the MD simulation [1], Catti [3] proposed an orthorhombic intermediate state with a $Pmm2$ symmetry, having a much lower activation energy than $R3m$. The space group of this intermediate state later was corrected to $Imm2$ because $Imm2$ is actually one of the maximal subgroups of the ZB structure [4]. Recent *ab initio* simulations [5] have shown that this orthorhombic intermediate state is a universal transition state for the ZB-to-RS transition in semiconductor compounds, indicating that the transition state is independent of their ionicity.

The ZB-to-RS phase change is a reconstructive phase transformation and it involves large atomic displacements. Therefore, the system can transform from one phase to another by passing through various closely related paths during the transition [6]. In other words, the transformation mechanism might follow various transition pathways or involve several intermediate states. Indeed, recent systematic group-theoretical analysis proposed several competitive low barrier pathways for the ZB-to-RS transformation of SiC in addition to the $Imm2$ phase [7]. In our earlier work, using a constant-pressure *ab initio* technique, we have shown that the ZB-to-RS phase change of SiC is based on both a tetragonal $I\bar{4}m2$ and orthorhombic ($Imm2$) intermediate state [8]. Such a tetragonal modification also formed in the classical MD simulation [1] but it was questioned in a first-principles calculation [6].

In this paper, we address the pressure-induced phase transition of ZnS using constant-pressure *ab initio* calculations. This material has been a subject of many experimental and theoretical studies [9–15]. A phase transition from the ZB structure to an RS structure has been reported around 14–19 GPa [9–12]. The RS phase remains stable up to 45 GPa, and a further increase of pressure leads to a transition into a disordered RS structure with $Cmcm$ symmetry. Upon pressure release, the RS crystal transforms back to the ZB state around 7 GPa [12].

Despite these extensive experimental and theoretical investigations, the transformation mechanism(s) from the ZB-to-RS structure in ZnS is(are) still unclear. Catti [16] argued that ZnS follows the same transformation mechanism of SiC even though ZnS is more ionic than SiC. Moreover, Miao and Lambrecht [6] shown that the transformation mechanism of the ZB-type compounds is independent of the chemical structure and is similar to that of SiC. However, to our knowledge a direct observation of the ZB-to-RS phase change in ZnS has not been reported in any simulations. Therefore, additional studies are basically needed to clarify the transformation mechanism in ZnS or to confirm the universal transition pathway in ZB-structured semiconductors. In this work, we perform a constant-pressure *ab initio* technique to study the behaviour of ZnS at high pressure. Particularly, we focus on the transformation pathway, intermediate states, and the role of nonhydrostatic conditions on the transformation mechanism during the phase change. We find that the transformation path observed in ZnS through the simulations is remarkably similar to that of SiC and hence our result strongly supports the universal transition state in the ZB structured semiconductors. Furthermore, we observe that the ZB-to-RS phase transition under nonhydrostatic compressions proceeds with a similar mechanism at least up to 10% stress deviation.

2. Methodology

We use the first-principles pseudopotentials method within the density-functional formalism and the local-density approximation using the Ceperley–Alder functional [17] for the exchange–correlation energy. The calculation is carried out with the *ab initio* program SIESTA [18] using a linear combination of atomic orbitals as the basis set, and norm-conservative Troullier–Martins Pseudopotential [19]. A split-valence double- ξ plus polarized basis set is employed. A uniform mesh with a plane wave cut-off of 150 Ryd is used to represent the electron density, the local part of the pseudopotentials, and the Hartree and the exchange–correlation potential. The simulation cell consists of 64 atoms with periodic boundary conditions. We use Γ -point sampling for the Brillouin zone integration, which is reasonable for a simulation cell with 64 atoms since the energy difference between a 64-atom simulation cell with only a Γ point and an 8-atom unit cell with 256 \mathbf{k} -points (see below) is less than 0.03 eV/atom. The molecular dynamical simulations are performed using the NPE ensemble. Pressure is applied via the method of Parrinello and Rahman [20] and increased with

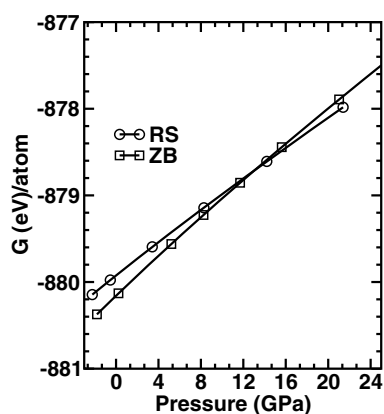


Figure 1. The computed Gibbs free-energy curve of the RS and ZB structures. The curves cross around 14.2 GPa, indicating a phase transition from the RS-to-ZB structure. The curves are guides to the eye.

an increment of 10 GPa with an equilibration period of 1000 time steps (each time step is one femtosecond (fs)).

For Gibbs free-energy calculations, on the other hand, we only consider only the unit cell (8 atoms) for both ZB and RS structures to reduce the computational effort. In order to sample the Brillouin zone, a set of 256 Monkhorst–Pack [21] special \mathbf{k} -points are used. Both structures are optimized at several volumes and then the Gibbs free energies at zero temperature are computed.

3. Results

3.1. Phase transition from Gibbs free energy

As we will discuss below, the predicted transition pressure in the Parrinello–Rahman simulations is generally overestimated and hence it is necessary to first consider energy–volume calculations and the thermodynamic criterion of equal free-energies in order to predict an accurate transition pressure for ZnS. The computed Gibbs free-energy curve of the ZB and RS structures is illustrated in figure 1. Accordingly, the curves cross around 14.2 GPa, indicating a first-order phase transition. This transition pressure is in excellent agreement with the experimental values of 14.7–18.1 GPa [9–12] and the previous theoretical results of 13.93–19.5 GPa [13–15].

We also fitted these data to the third-order Birch–Murnaghan equation of state to predict the structural parameters of both phases. The lattice constants of the ZB and RS structures are found to be about 5.3 and 5.01 Å, respectively, which are comparable with the previous theoretical results of 5.28–5.39 Å [11, 15, 22] for the ZB phase and 4.94–5.09 Å [11, 15, 22] for the RS phase, but slightly less than the experimental values of 5.41 Å (ZB) [23] and 5.06 Å (RS) [23]. Also the fitting yields 85.7 GPa for the bulk modulus of the ZB structure. This result is comparable with both the experimental and the theoretical values of 75.0–83.3 GPa [9–15]. For the RS phase, the bulk modulus is calculated to be 108.9 GPa, which is also in good agreement with the experimental and the theoretical results of 85.0–107.6 GPa [9–15]. A slight discrepancy between our results and the experimental data is related to some approximations used in the simulation scheme.

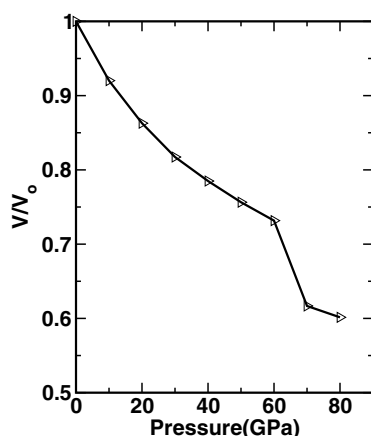


Figure 2. The pressure–volume curve of ZnS as a function of pressure from the Parrinello–Rahman simulation.

3.2. Parrinello–Rahman simulation

In order to characterize the thermodynamic nature of the phase transition of ZnS in the dynamical approach, we first plot the pressure volume relation in figure 2. Accordingly, the volume decreases gradually up to 70 GPa at which point a dramatic decline of the volume is seen, indicating a first-order phase transition in ZnS. The structural analysis reveals that, at 70 GPa, the ZB crystal transforms into an RS structure, in agreement with experiments. Upon fast pressure release from 70 to 0 GPa, a ZB phase is recovered. Therefore, the simulation technique successfully reproduces the reversible phase transition of ZnS. The transition pressure that lies between 60 and 70 GPa in the present simulation is, however, considerably larger than the experimental results of 14–18 GPa and the one predicted from Gibbs free-energy consideration of about 14.2 GPa in the previous section. Such a trend is generally seen in the Parrinello–Rahman simulations in which the transformation does not proceed by nucleation and growth, but instead it occurs across the entire simulation cell. As a result, the system has to cross a significant energy barrier to transform from one phase to another one, and hence the simulation box has to be overpressurized in order to obtain a phase transition within the accessible simulation time [24, 25].

The modification of the simulation cell during the phase transformation might provide a clear picture of the transformation mechanism in ZnS at the microscopic level. We plot the change of simulation cell lengths and angles at 70 GPa as a function of MD time step in figure 3. The simulation cell vectors **A**, **B**, and **C** are initially along the [100], [010] and [001] directions, respectively. The magnitude of these vectors is plotted in the figure. Accordingly, a simultaneous compression along the [010] direction of the ZB structure and an expansion along the other directions initially occur, and then the β -angle between **A** and **C** gradually changes gradually from 90° to about 70° , resulting in a monoclinic modification of the simulation cell during the phase transformation. Therefore, the ZB-to-RS phase change observed through the simulation in ZnS is due to the cubic \rightarrow tetragonal \rightarrow monoclinic adaptation of the simulation box. This mechanism is similar to that of SiC predicted in both *ab initio* [8] and classical MD simulations [1].

It is very important to determine the intermediate phases caused by this simple transformation mechanism. We can easily track the symmetry changes during the phase change

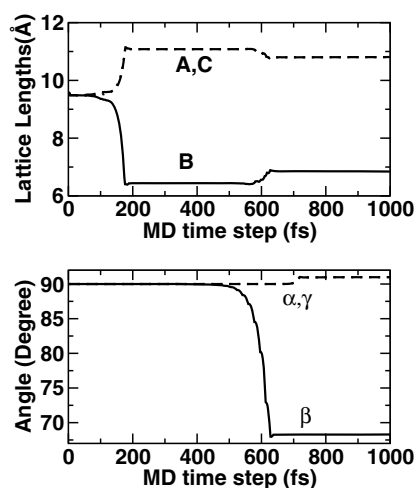


Figure 3. The time evolution of the simulation cell lengths and angles at 70 GPa.

Table 1. The atomic fractional coordinates and the lattice parameters of the phases formed at 70 GPa.

Phase	a (Å)	b (Å)	c (Å)	x	y	z
ZB $F\bar{4}3m$	4.7873	4.7873	4.7873	S: 0.0 Zn: 0.75	0.0 0.75	0.0 0.75
Tetragonal $I\bar{4}m2$	3.4631	3.4631	4.4384	S: 0.0 Zn: 0.0	0.0 0.0	0.75 0.5
Orthorhombic $Imm2$	4.0202	3.9181	3.2036	S: 0.0 Zn: 0.0	0.0 0.5	0.983 760 0.272 806
RS $Fm\bar{3}m$	4.5921	4.5921	4.5921	S: 0.5 Zn: 0.0	0.5 0.5038	0.5 0.5038

using the KPLOTT program [26] that provides detailed information about space group, cell parameters and atomic position of a given structure. Since the simulation cell is quite distorted during the transformation, we use 0.2 Å, 4°, and 0.7 Å tolerances for bond lengths, bond angles and interplanar spacing, respectively for the symmetry analysis. Around 150 fs, the cubic unit structure transforms into a tetragonal one with lattice parameters $a = b = 3.4631$ Å, and $c = 4.4384$ Å. The corresponding space group of the tetragonal unit cell is $I\bar{4}m2$. When the β -angle is about 86°, an orthorhombic unit cell with the space group $Imm2$ is formed and this is characterized by the unit cell constants $a = 4.0202$ Å, $b = 3.9181$ Å and $c = 3.2036$ Å. When the β -angle reaches a value of about 75°, the tetragonal angles are significantly opened and the simulation cell lengths are slightly modified again, which leads the neighbouring atoms to form a distorted RS structure in which the bond lengths and angles are not uniform. At later time steps, an almost perfect RS state with a lattice parameter of 4.5921 Å is gradually shaped due to the relaxation of the structure. The lattice constant of this RS structure, on the other hand, is considerably less than the experimental value of 5.06 Å [23], which is indeed related to the overpressurization of the simulation box. The lattice parameters and the atomic positions of the phases obtained at 70 GPa are summarized in table 1. We should note here that these parameters are certainly underestimated because of the overpressurization of the simulation cell.

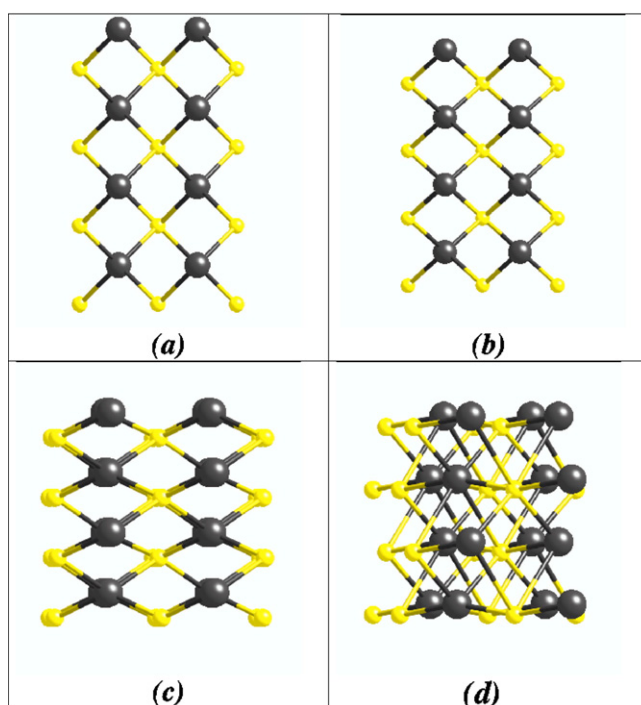


Figure 4. The evolution of the rock-salt structure at 70 GPa: (a) the zinc-blende structure at 1 fs; (b) the intermediate tetragonal phase at 150 fs; (c) the orthorhombic state at 565 fs; (d) the formation of the rock-salt structure at 611 fs.

(This figure is in colour only in the electronic version)

It is noteworthy that all previous enthalpy calculations strongly favour the orthorhombic $Imm2$ intermediate phase for the ZB-to-RS phase transformation. The tetragonal $I4m2$ state is however questioned in a first-principles method in which the calculation of the energy landscape indicates that there is no reason for the formation of the tetragonal phase [6]. The tetragonal adaptation may be related to the overestimated transition pressure in the Parrinello–Rahman simulation (because the different transition pressures can yield a different transition pathway) and/or the fast quenching artefact of the MD simulations. Even the monoclinic modification of the simulation cell might be due to these limitations, which can be only clarified experimentally by picosecond time-resolved electronic spectroscopy in shock wave experiments or by monitoring the shape changes of nanocrystals in ZB-type materials.

The relation between the simulation cell (64 atoms) and the unit cells are also determined using the KPLOT program. For the ZB structure, the unit cell vectors a , b and c are parallel to the simulation cell vectors A , B , and C and hence $a = A/2$, $b = B/2$, and $c = C/2$. With the modification to the tetragonal phase, the unit cell vectors become $a = -(A + C)/4$, $b = (-A + C)/4$, and $c = B/2$. The same relations hold for the orthorhombic state except that the signs of b and c are changed. For the RS phase, the unit cell vectors can be calculated using the following relations: $a = (A - 2B - C)/4$, $b = (A + 2B - C)/4$, and $c = (A + B)/4$.

A close analysis during the transformation reveals that the phase transition from the ZB-to-RS structures results from the distortion of tetrahedral angles and does not involve any bond breaking, in agreement with the previous observations [1, 8]. The simple transformation

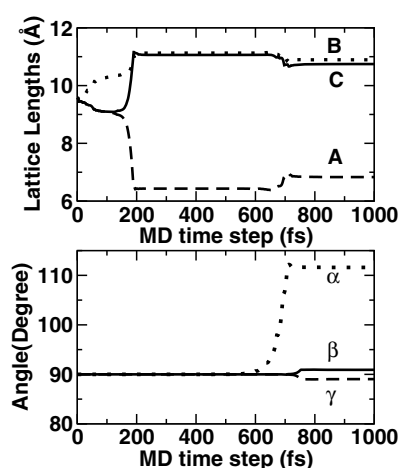


Figure 5. The simulation cell lengths and angles under nonhydrostatic compression at 70 GPa. The stress component along the [010] direction is decreased by 2% relative to the other components.

mechanism is illustrated in figure 4. For clarity, we show a small fragment of the simulation cell. During the transformation, the simulation cell length **B** ([010] direction in the ZB crystal) initially decreases to a small value while the other two perpendicular dimensions increase to a large value. Accompanied by this transformation, the Zn and S atoms shift against each other along the compressed direction. This forms the tetragonal phase. Note that simultaneous compression and expansions of the simulation cell produce the opening and closing of the tetragonal angles. With the monoclinic modification of the simulation cell, the tetragonal angles gradually tend toward 90° and 180° at which point an RS phase is formed. The opening of the tetrahedron leads to channels for the neighbouring atoms to form a sixfold-coordinated structure.

The transformation mechanism observed through the simulation so far is achieved under a perfect hydrostatic condition. In reality, the degree of the hydrostaticity in experiment is determined by the efficiency of the pressure-transmitting medium. At high pressures, the pressure-transmitting medium solidifies, resulting in strong nonhydrostatic effects. The role of stress deviations on the transformation mechanism, therefore, needs to be investigated. Here we consider two cases of nonhydrostatic compression only at 70 GPa: the stress component along the [010] direction is decreased by 2% and 10%. We choose this stress component because, in the perfect hydrostatic case, the structural phase change results from a dramatic reduction in this direction. Reducing stress components along the other directions probably encourages the structural transition since they are elongated during the phase change under the perfect hydrostatic pressure. However, a detailed analysis is indeed needed to clarify this issue. We should note here that our aim is to compare the transformation mechanism between the hydrostatic case and the nonhydrostatic cases and is not to accelerate or suppress the transformation.

For the case of 2% deviation, the system transforms into a RS structure by a compression of the [100]-axis and an increase of α -angle from 90° to about 110° as shown in figure 5. This transformation pathway is analogous to that found under the perfect hydrostatic condition. The 10% decrease in the stress factor is actually quite large and might be expected to play a significant role on the phase transformation and/or its mechanism. For this condition, the phase transition into an RS structure is suppressed in the accessible simulation time but the

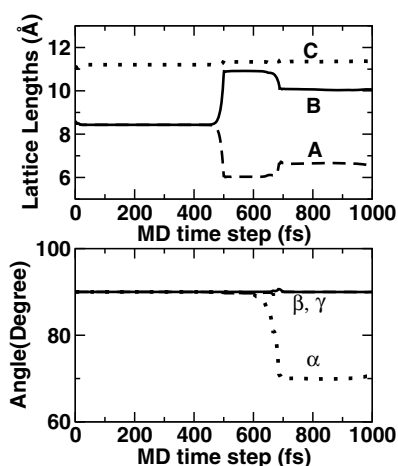


Figure 6. The simulation cell lengths and angles under nonhydrostatic compression at 90 GPa. The stress component along the [010] direction is decreased by 10% relative to the other components.

symmetry of the system is broken (a tetragonal phase with $I\bar{4}m2$ symmetry is formed with lattice parameters $a = b = 3.0347$ and $c = 5.5597$ Å) because of the nonhydrostaticity. In order to obtain a phase change, we increase the applied stress an increment of 10 GPa and equilibrate the system 1000 fs. A phase transition into an RS structure at 90 GPa occurs by a monoclinic modification of the simulation cell again (see figure 6). However, the elongated simulation cell lengths (B and C) in this nonhydrostatic situation do not have the same value, in contrast to the other cases (perfect hydrostatic and 2% stress deviation). This results in a distorted RS structure. Nevertheless, the transformation mechanism obtained in this nonhydrostatic environment is unexpectedly similar to what has been determined in the perfect hydrostatic condition, although the degree of nonhydrostatic compressions notably affects the transition pressure. Therefore, based on these observations, we reach a conclusion that the ZB-to-RS transition pathway of ZnS might be independent of the degree of nonhydrostatic conditions (up to 10% deviations) in the simulations. Definitely, detailed studies are more desirable to understand exactly the role of the stress deviations on this structural phase change and on its mechanism, since nonhydrostaticity can be applied by a variety of combinations.

4. Conclusions

We have studied the pressure-induced phase transition of ZnS using a constant-pressure *ab initio* technique. The method successfully reproduces the reversible phase transition from the ZB structure to an RS structure. Furthermore, the transformation mechanism and intermediate states are successfully characterized through the simulations. The phase change results from the monoclinic modification of the simulation cell and involves both a tetragonal $I\bar{4}m2$ and an orthorhombic $Imm2$ intermediate state. The transformation mechanism and intermediate states of ZnS are found to be similar to those of SiC even though ZnS is more ionic than SiC. These observations do indeed support the universal transition state of the high-pressure ZB-to-RS phase transition in semiconductor compounds. We also find that this mechanism is almost independent of the degree of the nonhydrostatic compression, at least up to 10% stress deviation, but further studies are actually needed to understand the function of stress deviations on phase transformations and their transition mechanism.

Acknowledgment

The calculations were run on an IBM eServer p690 machine acquired with the aid of an IBM Shared University Research Grant at the University of Texas at El Paso.

References

- [1] Shimojo F, Ebbsjö I, Kalia R, Nakano A, Rino J P and Vashista P 2000 *Phys. Rev. Lett.* **84** 3338
- [2] Karch K, Bechstedt F, Pavone P and Strauch D 1996 *Phys. Rev. B* **53** 13400
- [3] Catti M 2001 *Phys. Rev. Lett.* **87** 35504
- [4] Perez-Mato J M, Aroyo M, Capillas C, Blaha P and Schwarz K 2003 *Phys. Rev. Lett.* **90** 49603
- [5] Miao M S and Lambrecht W R L 2005 *Phys. Rev. Lett.* **94** 225501
- [6] Miao M S and Lambrecht W R L 2002 *Phys. Rev. B* **66** 64107
- [7] Hatch D M, Stokes H T, Dong J, Gunter J, Wang H and Lewis J P 2005 *Phys. Rev. B* **71** 184109
- [8] Durandurdu M 2004 *J. Phys.: Condens. Matter* **16** 4411
- [9] Smith P L and Martin J E 1965 *Phys. Lett.* **19** 541
- [10] Piermarini G J, Block S, Barnett J D and Forman R A 1975 *J. Appl. Phys.* **46** 2774
- [11] Ves S, Schwarz U, Christensen N E, Syassen K and Cardona M 1990 *Phys. Rev. B* **42** 9113
- [12] Desgreniers S, Beaulieu L and Lepage I 2000 *Phys. Rev. B* **61** 8726
- [13] Jaffe J E, Pandey R and Seel M J 1993 *Phys. Rev. B* **47** 6299
- [14] Recio J M, Pandey R and Luaña V 1993 *Phys. Rev. B* **47** 3401
- [15] Nazzal A and Qteish A 1996 *Phys. Rev. B* **53** 8262
- [16] Catti M 2002 *Phys. Rev. B* **65** 224115
- [17] Ceperley D M and Alder M J 1980 *Phys. Rev. Lett.* **45** 566
- [18] Ordejón P, Artacho E and Soler J M 1996 *Phys. Rev. B* **53** 10441
Sánchez-Portal D, Ordejón P, Artacho E and Soler J M 1997 *Int. J. Quantum Chem.* **65** 453
- [19] Troullier N and Martins J L 1997 *Phys. Rev. B* **43** 1993
- [20] Parrinello M and Rahman A 1980 *Phys. Rev. Lett.* **45** 1196
- [21] Monkhorst H J and Pack J D 1976 *Phys. Rev. B* **13** 5188
- [22] Qteish A, Abu-Jafar M and Nazzal A 1998 *J. Phys.: Condens. Matter* **10** 5069
- [23] Madelung O *et al* (ed) 1982 *Numerical Data and Functional Relationships in Science and Technology (Landolt-Börnstein New Series Group III, vol 17b)* (Berlin: Springer)
- [24] Mizushima K, Yip S and Kaxiras E 1994 *Phys. Rev. B* **50** 14952
- [25] Martoňák R, Laio A and Parrinello M 2003 *Phys. Rev. Lett.* **90** 75503
- [26] Hundt R, Schön J C, Hannemann A and Jansen M 1999 *J. Appl. Phys.* **32** 413